Characterization of the Ni-Zn/TiO$_2$ Nanocomposite Synthesized by the Liquid-Phase Selective-Deposition Method

Sarantuya Myagmarjav[1], Hideyuki Takahashi[2], Yoji Sunagawa[1], Katsutoshi Yamamoto[2], Nobuaki Sato[2], Eiichiro Matsubara[3] and Atsushi Muramatsu[2]

[1]*Graduate School of Environmental Studies, Tohoku University, Sendai 980-8577, Japan*
[2]*Institute for Multidisciplinary Research for Advanced Materials, Tohoku University, Sendai 980-8577, Japan*
[3]*Institute for Materials Research, Tohoku University, Sendai 980-8577, Japan*

The characterization of Ni-Zn/TiO$_2$ nanocomposite synthesized by the liquid-phase selective-deposition method was studied. Nanoparticles were well dispersed and stabilized by the selective deposition onto TiO$_2$ surface. The particle size was decreased with increasing the amount of Zn added, thus the catalytically active Ni surface area was increased. The selective deposition onto TiO$_2$ surface and addition of Zn to the nanoparticles promoted the catalytic activity of Ni-Zn nanoparticles, *e.g.* the catalytic activity of Ni-Zn/TiO$_2$ for 1-octene hydrogenation was ca. 10 times higher than that of the unsupported Ni nanoparticles. Ni in the nanocomposite was assigned as metallic, although their surface was oxidized under the atmospheric condition, but Zn and B were deposited as their oxide.

1. Introduction

Nanoparticles have been received much attention and been widely studied, since its property can change only by the size because of quantum effect when the size is reduced to nanometer level.[1] The decrease of the size is also expected to enhance the catalytic activity, because the decrease in size results in the increase of the total surface area. Among various methods to synthesize the nanometer-sized particles,[2–4] the liquid-phase reduction method is one of the easiest procedures, since nanoparticles can be directly obtained from various precursor compounds soluble in a specific solvent.[5] It has been reported that Ni and Ni-Zn nanoparticles with a diameter from 5 to 10 nm and an amorphous-like structure were synthesized by using liquid-phase reduction method and that Zn addition to Ni nanoparticles promote the catalytic activity for 1-octene hydrogenation.[6] However, unsupported particles lost their high activity due to tremendous aggregation because of its high surface activity.[7] In order to solve this problem, we have also reported their selective deposition method onto TiO$_2$ nanoparticles, named as the liquid-phase selective-deposition method.[8] In this paper, detailed characterization of Ni-Zn/TiO$_2$ nanocomposite will be reported.

2. Experimental

Nickel acetylacetonate (Ni(AA)$_2$·2H$_2$O, AA = CH$_3$CO-CHCOCH$_3$) and zinc acetylacetonate (Zn(AA)$_2$) were co-dissolved in 40 ml of 2-propanol with varying a Zn/Ni ratio from 0 to 1.0, where the amount of Ni(AA)$_2$ was 2.5×10^{-4} mol in constancy. 0.125 g of TiO$_2$ fine particles (Ishihara Ind., ST01) were dispersed in the Ni(AA)$_2$-Zn(AA)$_2$ solution in a 4-neck flask under refluxing conditions with a continuous N$_2$ flow for 30 min. Ni and Zn complexes were promptly reduced by the addition of 10 ml of 1.0×10^{-1} mol/dm^3 NaBH$_4$ 2-propanol solution. As prepared materials were recovered by filtration using a membrane filter with the pore size of 0.1 μm (ADVANTEC Co., Ltd.) and dried at room temperature for 24 hours in vacuum. Detailed synthesis method of Ni-Zn nanoparticles on the TiO$_2$ surface by the liquid-phase reductive-deposition method was already reported in Ref 8. Resultant solid was characterized by high-resolution transmission electron microscopy (HR-TEM, Hitachi Co., Ltd. HF-2000 field emission TEM) equipped with the electron energy loss spectroscopy detector (EELS), X-ray diffractometry (XRD, Rigaku Co., Ltd. RAD-IC system, CuKα 40 kV, 20 mA), FT-IR (Digilab Japan Co., Ltd. FTS7000/UMA600 system, 0.5%KBr pellet 100 mg), extended X-ray adsorption fine structure (EXAFS, Rigaku Co., Ltd. R-XAS Rooper), electron spectroscopy for chemical analysis (ESCA, ULVAC PHI ESCA 5600, Al Kα:45°, 3.0098×10^{-17} J (187.85 eV)) and Auger electron analysis. Residual concentration of Ni and Zn species in the filtrate was estimated by using an inductively coupled plasma atomic emission spectrometer (ICP, Shimadzu Co., Ltd. ICPS-1000 III) in order to evaluate the yield of Ni and Zn independently. The amount of B in the samples was estimated by ESCA and ICP.

The hydrogenation of 1-octene over as-prepared particles was carried out as a test reaction, since only the metallic Ni species can exhibit the catalytic activity in this reaction. Concretely, 1-octene was charged into 4-neck flask after the preparation of nanoparticles and then H$_2$ gas was introduced (1-octene, 5 ml; H$_2$ gas flow rate, 45 ml/min). The product in the liquid phase was analyzed by gas chromatography (GC, Shimadzu Co., Ltd. GC-14B system).

3. Results and Discussion

3.1 The size and catalytic activity of the Ni-Zn nanoparticle

Figure 1 shows the TEM micrographs of Ni and Ni-Zn (Zn/Ni = 1.0) nanoparticles in the presence of TiO$_2$ supports (a) and its absence (b). The size of Ni and Ni-Zn nanoparticles formed without TiO$_2$ supports was 5–10 nm and the tremendous aggregation was found. On the other hand, it
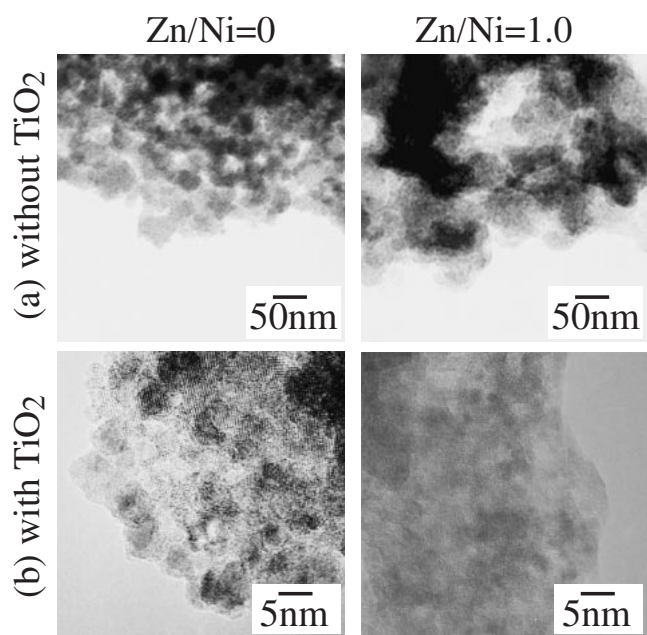
Zn/Ni=0   Zn/Ni=1.0

(a) without TiO$_2$

50nm   50nm

(b) with TiO$_2$

5nm   5nm

Fig. 1   TEM micrographs of Ni and Ni-Zn nanoparticles in the absence of TiO$_2$ (a) and its presence (b).

clearly demonstrated that Ni and Ni-Zn nanoparticles were completely selectively deposited on TiO$_2$ surface for supported materials. In addition, no nanoparticle was found irrespectively apart from TiO$_2$ surface. The size of Ni-Zn nanoparticles deposited on TiO$_2$ surface was decreased from 5–6 nm (Zn/Ni = 0) to 1 nm (Zn/Ni = 1.0) with increasing

the amount of Zn added.

The catalytic activities of Ni and Ni-Zn (Zn/Ni = 1.0) nanoparticles with and without TiO$_2$ supports were evaluated through 1-octene hydrogenation. The GC analyses confirmed that only *n*-octane was obtained as a product in this hydrogenation reaction. The conversion activity of unsupported particles was 4% (Ni nanoparticle) and 11% (Ni-Zn nanoparticle), while that of TiO$_2$ supported materials was increased to 21% (Ni/TiO$_2$) and 40% (Ni-Zn/TiO$_2$). Taking into the consideration of the fact that conversion from 1-octene to *n*-octane can occur only at the metallic Ni surface and not at Ni oxide, the state of Ni species in the nanocomposite may be metallic. The catalytic activity of Ni-Zn/TiO$_2$ was ca. 10 times higher than that of the unsupported Ni nanoparticles. These results imply that TiO$_2$ plays an important role to disperse and stabilize the nanoparticles by the selective deposition on its surface. Also, the addition of Zn clearly increases in the catalytically active Ni surface, since the Zn addition resulted in the decrease in the particle size. These effects promote the catalytic activity of the nanoparticles. However, the valence of Ni, Zn and B as by-product in the nanoparticles was still unclear until now. Therefore, Ni-Zn nanoparticles on TiO$_2$ were characterized by ESCA, EXAFS and Auger electron analysis.

3.2   The valence of Ni, Zn and B in the Ni-Zn/TiO$_2$ nanocomposite

3.2.1   The valence of the Ni

Ni nanoparticles deposited on TiO$_2$ were characterized by ESCA and EXAFS. Figure 2 shows ESCA spectra of Ni

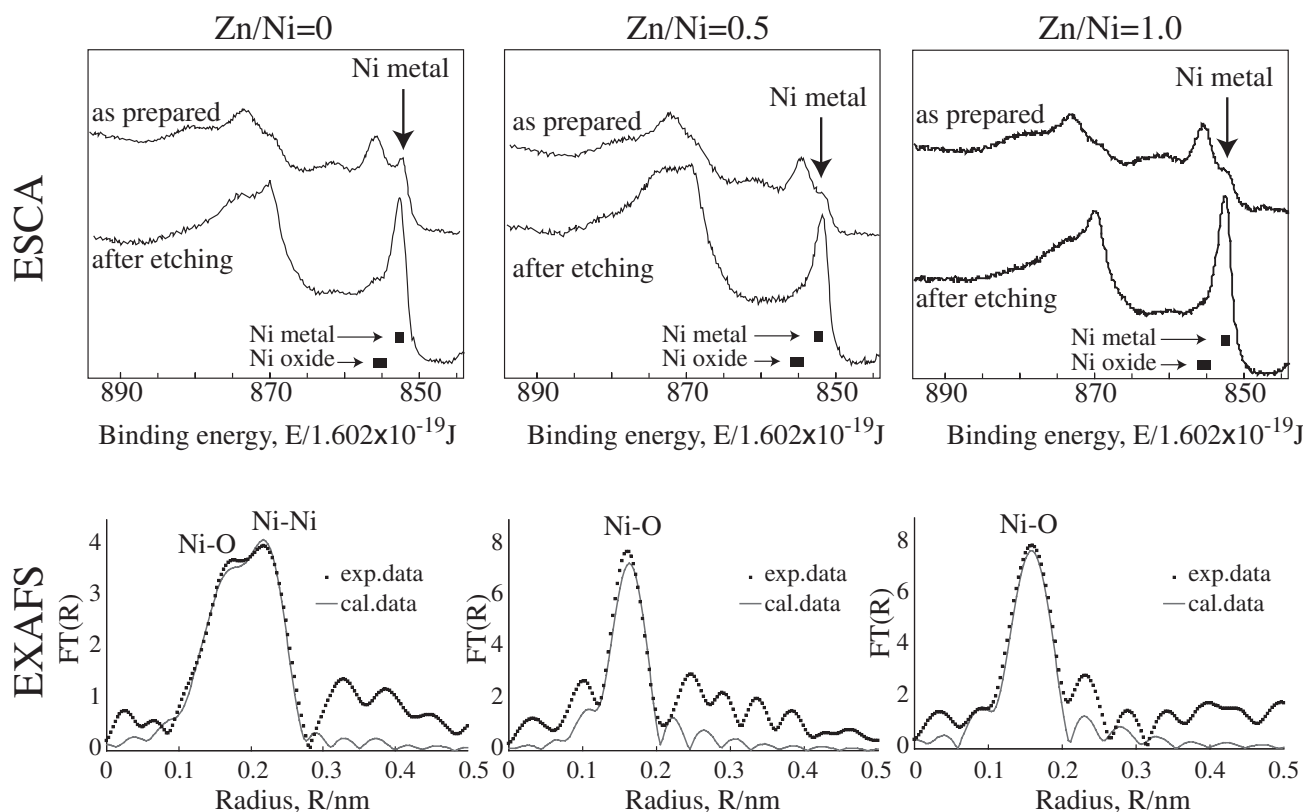Zn/Ni=0   Zn/Ni=0.5   Zn/Ni=1.0

ESCA

Ni metal   Ni metal   Ni metal
as prepared   as prepared   as prepared

after etching   after etching   after etching

Ni metal →   Ni metal →   Ni metal →
Ni oxide →   Ni oxide →   Ni oxide →

890   870   850   890   870   850   890   870   850

Binding energy, E/1.602x10^{-19}J   Binding energy, E/1.602x10^{-19}J   Binding energy, E/1.602x10^{-19}J

EXAFS

Ni-Ni   Ni-O   Ni-O
Ni-O
FT(R)   FT(R)   FT(R)
· exp.data   · exp.data   · exp.data
— cal.data   — cal.data   — cal.data

0 0.1 0.2 0.3 0.4 0.5   0 0.1 0.2 0.3 0.4 0.5   0 0.1 0.2 0.3 0.4 0.5
Radius, R/nm   Radius, R/nm   Radius, R/nm

Fig. 2   ESCA spectra for the Ni 2p$_{3/2}$ region before and after etching and EXAFS profiles at Ni k-edge of Ni-Zn/TiO$_2$ nanocomposite prepared at Zn/Ni = 0, 0.5 and 1.0.
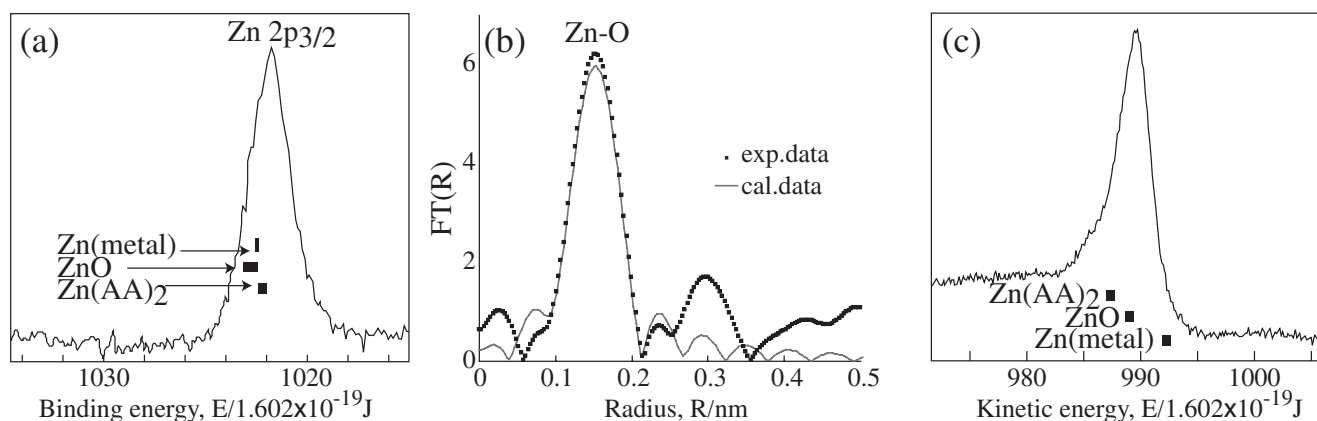
Fig. 3 (a) ESCA spectrum for the Zn 2p$_{3/2}$ region, (b) EXAFS profile at Zn k-edge and (c) Auger spectrum of Zn LMM region in the case of Zn/Ni = 1.0.

2p$_{3/2}$ region, before and after Ar$^+$ etching, and EXAFS profiles at Ni K-edge of (a) Ni (Zn/Ni = 0), (b) Ni-Zn (Zn/Ni = 0.5) and (c) Ni-Zn (Zn/Ni = 1.0) nanoparticles on the surface of TiO₂. From the ESCA spectra of as-prepared samples in each case, two peaks corresponding to Ni oxide (855.4 × 1.602 × 10^{-19} J) and Ni metal (852.1 × 1.602 × 10^{-19} J) were observed, while Ni metal was predominant after etching with Ar$^+$ for 1 min in each case.[9–11] For EXAFS of Zn/Ni = 0, the Ni-O and Ni-Ni peaks are clearly observed, while for the Zn/Ni = 0.5 and 1.0, only the Ni-O is observed. The peaks originated from 2nd neighbor, such as Ni-Ni-Ni, can not be found in every case, possibly because Ni-Ni and Ni-O bonds are formed only in short range, as we have been reported the nanoparticles have amorphous like structure.[12] As a result, the initial state of Ni in the nanoparticles must be metallic, although their surface was oxidized under the atmospheric condition. The peak of Ni metal can found from the ESCA analysis in every Zn/Ni ratio, while Ni-Ni peak can not be apparently observed in the EXAFS spectra of Zn/Ni = 0.5 and 1.0. Taking the results of catalytic activity measurement into consideration, the valence of Ni in the nanocomposite must be metallic for Zn/Ni = 0.5 and 1.0. Thus, in the EXAFS spectra for Ni-Zn/TiO₂ nanocomposite with Zn/Ni = 0.5 and 1.0, the peak of Ni-O formed at the surface of nanoparticles may be strongly observed than the peak of Ni-Ni formed inside the nanoparticles, because of small particle size (~1 nm) and amorphous structure.

3.2.2 The valence of the Zn

Figures 3(a), (b) and (c) shows the ESCA spectrum of Zn 2p$_{3/2}$ region, EXAFS profile at the Zn K-edge and Auger spectrum of Zn LMM region in the case of Zn/Ni = 1.0, respectively. From the ESCA spectrum, only the broad peak was observed. However, it difficult to decide the valence of Zn from ESCA analysis, since the peak position of Zn metal and Zn oxide was almost same.[9,13,14] From the result of EXAFS analysis, Zn-O was clearly observed. Also, from the Auger electron analysis, broad peak corresponding to Zn oxide (989.875 × 1.602 × 10^{-19} J) was observed. Thus, the valence of Zn in the nanoparticles must be oxide.

3.2.3 The valence of the B

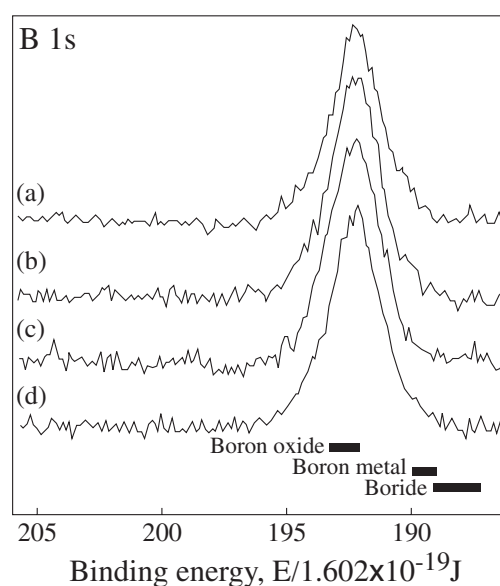Figure 4 shows the ESCA spectra of B 1s region of (a) as-prepared Ni/TiO₂, (b) Ni/TiO₂ after Ar$^+$ etching, (c) as-

Fig. 4 ESCA spectra of B 1s region of (a) as-prepared Ni/TiO₂, (b) Ni/TiO₂ after Ar$^+$ etching, (c) as-prepared Ni-Zn/TiO₂ (Zn/Ni = 0.5) and (d) Ni-Zn/TiO₂ (Zn/Ni = 0.5) after Ar$^+$ etching.

prepared Ni-Zn/TiO₂ (Zn/Ni = 0.5) and (d) Ni-Zn/TiO2 (Zn/Ni = 0.5) after Ar$^+$ etching. In any case, only the broad peak corresponding to B oxide was observed,[15,16] nevertheless the samples was etched with Ar$^+$ in the case of (b) and (d). Thus, the valence of B must not be metallic but oxide. Also, the addition of Zn was not affected to the valence of B. In our previous report,[8] the valence of the B was unclear ether "boride", since the ratio of B and Ni in the sample was close to Ni₃B and also the fact that Ni boride is easily formed[17] or "oxide" as the by-product, since B content was decreased by washing with water. From the analysis of the valence of Ni, Zn and B in this study, there was no evidence of the bonds between B and Ni or Zn. In addition, the peak of B oxide was clearly observed from the ESCA analysis. Therefore, B was formed as its oxide.

From these results, Ni must be metallic with surface oxidized in the atmospheric condition, and Zn and B was formed as their oxide. The deposition recovery of Ni and Zn onto TiO₂ was calculated as 99% and 97%, respectively from

the ICP measurement of supernatant solutions. On the other hand, B was also detected in nanoparticles deposited on TiO_2. Namely, the B/Ni ratio was evaluated to be 26.7/73.3 for $Zn/Ni = 0$ and 39.4/60.6 for $Zn/Ni = 1.0$ from the ESCA analysis. Also, residual amount of B was confirmed in the filtrates from the ICP measurement. The reason why B content in the samples was increased with increase in the amount of $Zn(AA)_2$ cannot be explained by the formation of metal boride, since Zn boride could not be formed in the present conditions. Virtually, there was no evidence of any boride formation. Zn addition decreased the particle size of Ni nanoparticles, or increased their surface area. Taking this fact into consideration, it can be concluded that $Zn(AA)_2$ must be selectively adsorbed on Ni nanoparticles, and hydrolyzed together with $NaBH_4$ after its addition. Alternatively, formed ZnO can promote the decomposition of $NaBH_4$ to form B oxides.

4. Conclusion

The catalytic activity of Ni-Zn nanoparticle was promoted by the selective deposition onto TiO_2 surface, since TiO_2 plays an important role to disperse and stabilize the nanoparticles. Also, the addition of Zn clearly promoted the hydrogenation activity of Ni, since the Zn addition resulted in inhibition against the growth of the size, thus, the increase in the catalytically active Ni surface area. The valence of the Ni in the Ni-Zn/TiO_2 nanocomposite was assigned as metallic, although their surface was oxidized under the atmospheric condition, and Zn and B in the nanocomposite is formed as their oxide.

REFERENCES

1) R. Kubo: J. Phys. Soc. Jpn. **17** (1962) 975–980.
2) P. N. Barnes, P. T. Murray, T. Haugan, R. Rogow and G. P. Perram: Physical C-Superconductivity and its Applications **377** (2002) 578–584.
3) K. Wegner, B. Walker, S. Tsantilis and S. E. Pratsinis: Chem. Eng. Sci. **57** (2002) 1753–1762.
4) B. Xia, K. Okuyama and I. W. Lenggoro: Adv. Mater. **13** (2001) 1744–1744.
5) A. Muramatsu and Y. Waseda: in *Morphology Control of Materials and Nanoparticles*, Y. Waseda and A. Muramatsu, Ed., (Springer-Verlag, Berlin, 2003) 129–149.
6) A. Muramatsu, S. Shitara, H. Sasaki and S. Usui: Shigen-to-sozai **106** (1990) 805–810.
7) H. Takahashi, A. Muramatsu, E. Matsubara and Y. Waseda: Shigen-to-sozai **118** (2002) 211–216.
8) H. Takahashi, Y. Sunagawa, S. Myagmarjav, K. Yamamoto, N. Sato and A. Muramatsu: Mat. Trans. **44** (2003) 2414–2416.
9) A. Lebugle, U. Axelsson, R. Nyholm and N. Martensson: Phys. Scr. **23** (1981) 825–827.
10) T. Dickinson, A. F. Povey and P. M. A. Sherwood: J. Chem. Soc. Faraday Trans. **173** (1977) 332–343.
11) K. Ng and D. M. Hercules: J. Phys. Chem. **80** (1976) 2095–2098.
12) H. Takahashi, Y. Sunagawa, S. Myagmarjav, K. Yamamoto, N. Sato and A. Muramatsu: Proceedings of the Fourth International Conference on Intelligent Processing and Manufacturing of Materials, (2003) CD-ROM.
13) G. Shoen: J. Electron Spectrosc. Relat. Phonom. **2** (1973) 75.
14) C. D. Wagner: Discuss. Faraday. Soc. **60** (1975) 291.
15) D. N. Hendrickson, J. M. Hollander and W. L. Jolly: Inorg. Chem. **9** (1970) 612.
16) W. A. Brainard and D. R. Wheeler: J. Vac. Soc. Technol. **15** (1978) 1801.
17) A. Furster. eds, Active Metal. (1996) 340–341.